J Appl Electrochem (2013) 43:689–696
DOI 10.1007/s10800-013-0554-1

ORIGINAL PAPER

Electrochemical determination of malachite green at graphene quantum dots–gold nanoparticles multilayers–modified glassy carbon electrode

Juying Hou · Feng Bei · Minglin Wang · Shiyun Ai

Received: 4 March 2013 / Accepted: 29 April 2013 / Published online: 23 May 2013

Abstract A graphene quantum dots–gold nanoparticles–modified glassy carbon electrode was used to investigate the electrochemical behaviors of malachite green (MG). Cyclic voltammetry curves of MG at the modified electrode exhibited a pair of quasi-reversible adsorption-controlled redox peaks at 0.502 V (E_{pa}) and 0.446 V (E_{pc}) in a 0.05 mol L^{-1} H_2SO_4 solution. Under the optimal conditions, by using differential pulse voltammetry as the detection method, a linear relationship was obtained between the oxidation peak current and the MG concentration in the range of 4.0×10^{-7} to 1.0×10^{-5} mol L^{-1} with the detection limit as 1.0×10^{-7} mol L^{-1} (signal-to-noise ratio of 3). The modified electrode was applied in the determination of MG in fish samples, and the results were satisfactory with recoveries from 96.25 to 98.00 %. Furthermore, the modified electrode showed very good reproducibility and stability.

Keywords Malachite green · Graphene quantum dots · Gold nanoparticles · Modified electrode · Electro-oxidation

J. Hou · M. Wang (✉)
College of Food Science and Engineering, Shandong Agricultural University, Taian 271018, Shandong, People's Republic of China
e-mail: mlwang@sdau.edu.cn

J. Hou · S. Ai (✉)
College of Chemistry and Material Science, Shandong Agricultural University, Taian 271018, Shandong, People's Republic of China
e-mail: chemashy@yahoo.com.cn; ashy@sdau.edu.cn

F. Bei
Taian Entry–Exit Inspection and Quarantine Bureau, Taian 271018, Shandong, People's Republic of China

1 Introduction

The use of malachite green (Scheme 1a) has been widespread as colorants in industry and as antimicrobial agents due to low cost and ready availability. Since 1990, researchers have found that this azo dye is highly toxic, carcinogenic, and mutagenic [1–3]. Therefore, it is very significant to monitor malachite green in aquatic products.

Quantitative analysis of malachite green in fish tissue today is usually performed by liquid chromatography, and liquid chromatography with mass and tandem mass spectrometry [4–6]. In the recent years, immunoassay method has also been used as a rapid, specific, and sensitive method [7–9]. These approaches possess high sensitivity and excellent selectivity. However, these methods require expensive instruments and time-consuming pretreatment processes. Electrochemical methods are alternative quantitative methods and have received an increasing attention in the detection of harmful residues, due to its high sensitivity, good selectivity, rapid response, and low cost. Up to date, the electrochemical determination of MG is rarely reported [10]. So, new modified electrodes with good catalytic performance for the determination of MG are still needed. Graphene is a two-dimensional honeycomb network of sp^2-hybridized carbon atoms [11]. Due to the remarkable conductivity, high surface-to-volume ratio, and good biocompatibility, several works of electrochemical sensors and biosensors have been introduced based on graphene materials [12, 13]. Graphene sheets, which are smaller than 100 nm, are called graphene quantum dots (GQDs). Owing to quantum confinement and edge effects, GQDs have various electronic and optoelectronic properties and can be an excellent candidate for construction of electrochemical sensor. A few of electrochemical sensors constructed with GQDs have been reported [14, 15]. It has

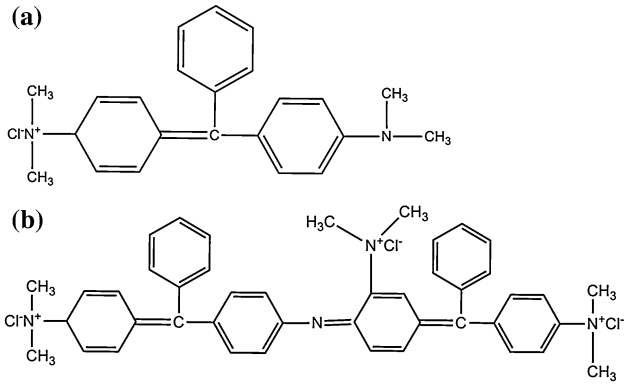

Scheme 1 Chemical structures of MG (**a**) and PMG (**b**)

been reported that the integration of carbon-based materials and metal nanoparticles [16, 17] can offer synergistic effect in electrocatalytic applications. The carbon-based materials can provide an ideal graphitic carbon surface for the assembly, dispersion, and stabilization of metal nanoparticles. So we have reason to expect the GQDs–Au composite would have the same effect.

In this study, a new graphene quantum dots–gold nanoparticles multilayers–modified glassy carbon electrode was successfully fabricated to detect MG. Its preparation involved two steps: (1) Electrodes were modified with GQDs and (2) electrodes were electrodeposited with Au nanoparticles in a $HAuCl_4$ solution. By layer-by-layer methods, the anodic potential of MG was reduced and the anodic current was obviously increased.

2 Experimental

2.1 Reagents and apparatus

High-purity graphite rods were purchased from the Qingdao Tennry Carbon Co. (China). Malachite green was obtained from Tianjin Basf Chemical Co., Ltd. (China). By dissolving 146.0 mg of MG into 100.0 mL redistilled deionized water, 4 mmol L^{-1} of MG stock solution was prepared. Chloroauric acid and sulfuric acid were purchased from Pure Crystal Reagent Ltd. (China) and used as received. Other chemicals were of analytical reagent grade, and all the solutions were prepared with redistilled deionized water. Phosphate-buffered saline (PBS) was prepared by dissolving 8.94 g sodium chloride, 0.77 g disodium hydrogen phosphate, and 0.18 g potassium dihydrogen phosphate in 1,000 mL redistilled deionized water and adjusted to the proper pH 7.4 using 1 mol L^{-1} hydrochloric acid and 1 mol L^{-1} sodium hydroxide.

Electrochemical experiments were performed with CHI 660C electrochemical workstation (Shanghai Chenhua Co., China) with a conventional three-electrode cell. The working electrode is a bare glassy carbon electrode ($d = 3$ mm, GCE) or modified glassy carbon electrode. A saturated calomel electrode (SCE) and a platinum wire were used as reference electrode and auxiliary electrode, respectively. The differential pulse voltammetry (DPV) was carried out with the parameters of increment potential, 0.004 V; pulse amplitude, 0.05 V; pulse width, 0.05 s; sample width, 0.0167 s; pulse period, 0.2 s; and quiet time, 2 s. The transmission electron microscope (TEM) image was obtained at JEM-2100TEM (Japan). The scanning electron microscopy (SEM) was performed on a Hitachi S-3000 N instrument (Japan).

2.2 Preparation of GQDs

GQDs were prepared according to the previous report [18]. Briefly, graphene oxide sheets were prepared from natural graphite powder by a modified Hummers method [19, 20]. Micrometer-sized graphene sheets (GSs) were obtained by thermal deoxidization of graphene oxide sheets in a tube furnace at 200–300 °C for 2 h with a heating rate of 5 °C min^{-1} in nitrogen atmosphere. GSs (0.05 g) were oxidized in a concentrated H_2SO_4 (10 mL) and HNO_3 (30 mL) mixed solution for 20 h under mild ultrasonication (500 W, 40 kHz). The mixture was then diluted with deionized water (250 mL) and filtered through 0.22-μm microporous membrane to remove the acids. Purified oxidized GSs (0.2 g) were redispersed in deionized water (40 mL), and the pH was adjusted to 8 with NaOH (1 mol L^{-1}). The suspension was transferred to a poly(tetrafluoroethylene) autoclave (50 mL) and heated at 200 °C for 10 h. After cooling to room temperature, the resulting black suspension was filtered through a 0.22-μm microporous membrane and a brown filter solution was separated. The colloidal solution still contained some large graphene nanoparticles (50–200 nm). So, the colloidal solution was further dialyzed in a dialysis bag (retained molecular weight 3,500 Da) overnight.

2.3 Fabrication of modified electrodes

Before modification, the bare GCE was polished to mirror with 0.3 and 0.05 μm alumina slurry on microcloth pads, rinsed thoroughly with redistilled deionized water, and then washed successively with anhydrous alcohol and redistilled deionized water in an ultrasonic bath, respectively. Finally, it was dried in air before use. For preparation of modified electrode, 2 mg mL^{-1} GQDs solution was first prepared by dispersing GQDs in redistilled deionized water, following ultrasonication for 1 h. With a microinjector, 10 μL of GQDs solution was dropped on the surface of GCE to obtain GQDs/GCE. The electrodeposition of Au nanoparticles at

the GQDs/GCE was performed in a $HAuCl_4$ (3 mmol L^{-1}) solution by applying a negative potential of −0.2 V (vs. SCE) for 100 s, which was negative enough for the electrochemical reduction of chloroauric acid to Au nanoparticles. Multilayers of GQDs/Au were then constructed by repeated alternative dropping of the GQD solution and electrodeposition of Au nanoparticles. The modified electrode was denoted in the text as $(GQDs/Au)_n$/GCE where n stands for the number of bilayers. Au/GCE was constructed by direct electrodeposition of Au nanoparticles at the GCE. The modified GCE was stored at 4 °C in a refrigerator when it was not in use. The same cleaned procedure was applied to the electrode before it was modified every time.

2.4 Preparation of fish sample

The salmon was purchased from local supermarket. The fish samples were prepared according to the previous report [9]. The fish was filleted, the skin and bones were removed, and the muscles were minced and deep-frozen before the detection. To the muscle samples (2 g), 10 μL MG solution (4 mmol L^{-1}) was added. Samples were allowed to equilibrate for 15 min before extraction. The sample was mixed with 4 mL 2 mol L^{-1} NaCl in PBS 7.4 by a vortex mixing for 1 min. Afterward, 2 mL HCl solution (1 mol L^{-1}) was mixed with the sample by another vortex mixing for 1 min. After centrifugation (2,000 rpm, 5 min), 4 mL solution was pipetted from underneath the fat layer into a tube and 5 mL dichloromethane was added. The tube was shaken overhead for 1 min. After centrifugation for 5 min, at 2,000 rpm, 5 mL of the upper layer was removed. Three milliliters of the dichloromethane phase was pipetted into a 10-mL glass tube and evaporated with nitrogen until dried at 50 °C. Residues were dissolved with 25 mL 100 % methanol. Further, 10 mL 0.05 mol L^{-1} H_2SO_4 solution was added and mixed by a vortex mixing for several minutes. The attained solution was used as DPV detection.

3 Results and discussion

3.1 Characterization of GQDs and surface morphological studies on GQDs/Au multilayers

Figure 1a showed the TEM image of the colloidal solution of GQDs. Their diameters are mainly distributed in the range of 5–15 nm (average diameter 10 nm). From Fig. 1a, it can be seen that most of GQDs were uniformly dispersed, and a small amount of GQDs aggregated. Figure 1b showed the SEM image of $(GQDs/Au)_1$ multilayers. The diameters of gold nanoparticles are mainly distributed in the range of 150–300 nm.

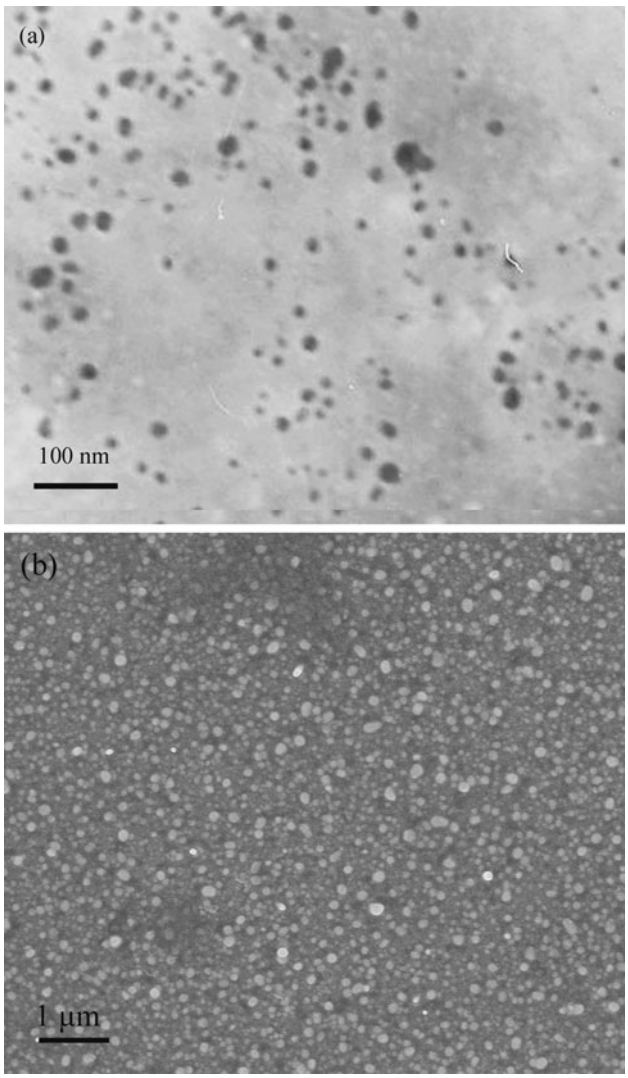

Fig. 1 **a** TEM image of GQDs. **b** SEM image of $(GQDs/Au)_1$ multilayers

3.2 Characterization of electrochemical behavior of $(GQDs/Au)_n$/GCE

Cyclic voltammograms of 5 mmol L^{-1} $Fe(CN)_6^{3-/4-}$ at GCE (a), GQDs/GCE (b), $(GQDs/Au)_1$/GCE (c), and $(GQDs/Au)_4$/GCE (d) were shown in Fig. 2. A couple of well-defined redox peaks were observed at bare GCE with peak-to-peak separation (ΔE_p) of 98 mV. But when the electrode was coated with GQDs, an increase in ΔE_p and a decrease in peak current (I_p) were observed. This phenomenon indicated there were electrostatic repulsive interactions between GQDs and $[Fe(CN)_6]^{3-/4-}$ anions. But when the electrode was coated with Au nanoparticles, an obvious increase in peak current was observed. This observation proved that the modified electrode showed fine catalytic activity. Furthermore, the current signal at the

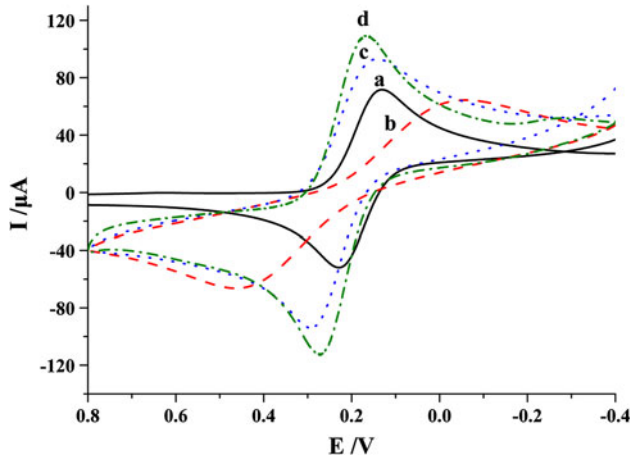

Fig. 2 Cyclic voltammograms of 5 mmol L^{-1} $Fe(CN)_6^{3-/4-}$ (1:1) in 0.1 mol L^{-1} KCl solution recorded at GCE (*a*), GQDs/GCE (*b*), $(GQDs/Au)_1$/GCE (*c*), and $(GQDs/Au)_4$/GCE (*d*). Scan rate: 100 mV s^{-1}

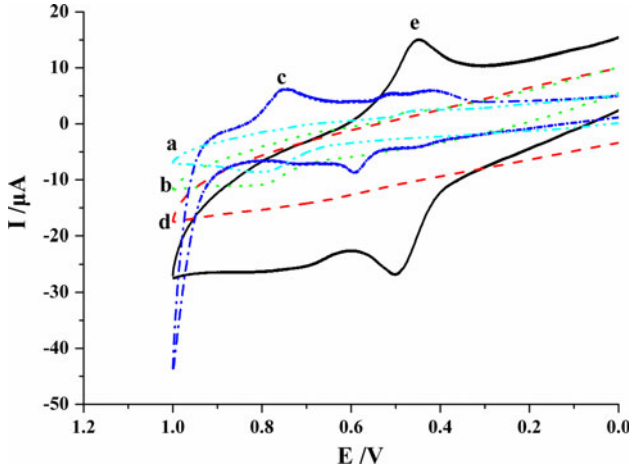

Fig. 3 Cyclic voltammograms of GCE (*a*), GQDs/GCE (*b*), Au/GCE (*c*), and $(GQDs/Au)_4$/GCE (*d*, *e*) in the absence (*d*) and presence (*a–c*, *e*) of 4.0×10^{-5} mol L^{-1} MG in 0.05 mol L^{-1} H_2SO_4 solution. Scan rate: 100 mV s^{-1}

$(GQDs/Au)_4$/GCE was stronger than at the $(GQDs/Au)_1$/GCE.

3.3 Cyclic voltammetric behaviors of MG

Figure 3 showed cyclic voltammograms of GCE (a), GQDs/GCE (b), Au/GCE (c), and $(GQDs/Au)_4$/GCE (d, e) in the presence (a–c, e) and absence (d) of 4.0×10^{-5} mol L^{-1} MG in 0.05 mol L^{-1} H_2SO_4 solution at a scan rate of 100 mV s^{-1}. When MG was absent, no redox peak was observed at the $(GQDs/Au)_4$/GCE, suggesting that GQDs and Au nanoparticles were electroinactive in the selected potential region. The peaks of oxidation and reduction appeared 0.502 and 0.446 V, respectively, at the $(GQDs/Au)_4$/GCE. The redox reaction may be the mutual transform of MG and poly(malachite green) (PMG) (Scheme 1b) [21–26]. The oxidation peak current at the $(GQDs/Au)_4$/GCE was about 2 times higher than at the GQDs/GCE in 4.0×10^{-5} mol L^{-1} MG. The reduction peak current at the $(GQDs/Au)_4$/GCE was about 5 times higher than at the GQDs/GCE. This observation may be attributed to the synergistic effects of GQDs and Au nanoparticles.

3.4 Optimization parameters

3.4.1 Influence of the number of bilayers

The effect of the number of bilayers on the oxidation of MG was investigated by DPV. Figure 4 showed the effect of the number of bilayers on the oxidation of MG. It revealed that the oxidation peak current increased gradually up to the number of films 4 and then decreased. The oxidation peak current at the $(GQDs/Au)_4$/GCE was about 2 times higher than at the $(GQDs/Au)_1$/GCE in 1.0×10^{-5} mol L^{-1} MG. This observation may be attributed to two aspects: With the increasing of n, the effective surface area of the electrode increased; at the same time, the electron transfer resistance increased.

3.4.2 Influence of accumulation time

The effect of accumulation time on the oxidation of MG was investigated by DPV. Figure 5 illustrated the relationship between the oxidation peak current of MG and accumulation time under open-circuit condition. The oxidation peak current increased gradually with accumulation time up to 400 s and then leveled off. This phenomenon could be attributed to saturated adsorption of MG at the

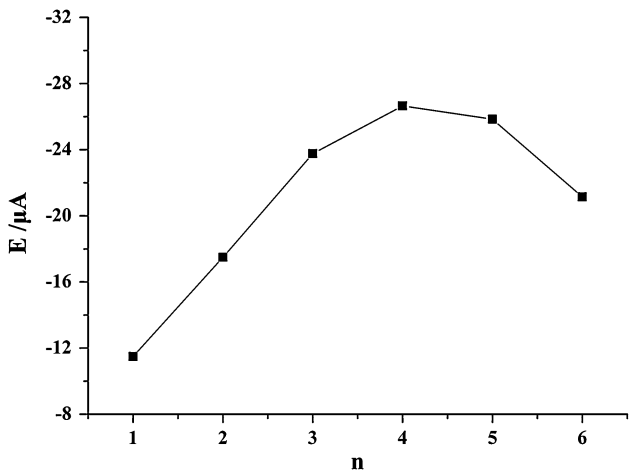

Fig. 4 Influence of the number of bilayers on the oxidation response of 1.0×10^{-5} mol L^{-1} MG at the modified electrode. Accumulation time: 400 s; open-circuit accumulation

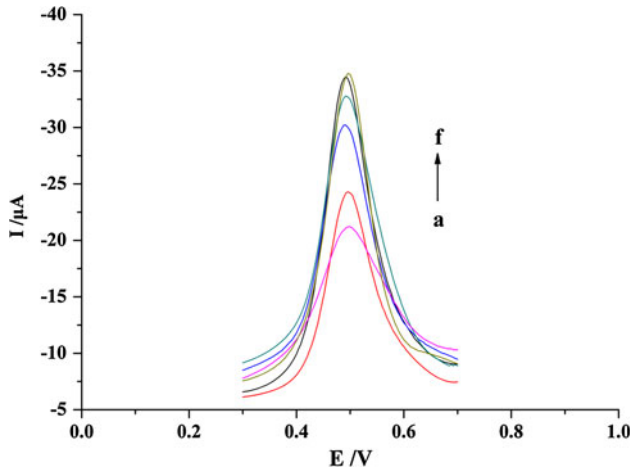

Fig. 5 Differential pulse voltammograms of 1.0×10^{-5} mol L^{-1} MG in 0.05 mol L^{-1} H_2SO_4 solution at the $(GQDs/Au)_4$/GCE at different accumulation time (from *a* to *f*: 0, 100, 200, 300, 400, and 500 s) under open-circuit condition

modified electrode surface. So, in the following experiments, the accumulation time was fixed at 400 s.

3.4.3 Influence of scan rate

The influence of scan rate on the electrochemical responses of MG was studied by cyclic voltammetry, and the results were shown in Fig. 6a. Fig. 6b showed the peak current increased linearly with the scan rate in the range of 40 to 800 mV s^{-1} and the linear regression equation was calculated as follows: $I_{pa} = -0.0853\ v - 6.817$ (μA, mV s^{-1}, $R = 0.998$), $I_{pc} = 0.0737\ v + 4.080$ (μA, mV s^{-1}, $R = 0.998$). The result indicated that electrode process was controlled by adsorption.

From Fig. 6c, it can be seen that E_{pa} changed linearly versus ln*v* with a linear regression equation of $E_{pa} = 0.0595 \log v + 0.5413$ (V, mV s^{-1}, $R = 0.994$), and E_{pc} changed linearly versus ln*v* with a linear regression equation of $E_{pc} = -0.063 \log v + 0.4112$ (V, mV s^{-1}, $R = 0.993$), in the range of 300 to 800 mV s^{-1}. According to the following Eq. (1) [27], the anodic and cathodic peak potentials were linearly dependent on the logarithm of the scan rates (*v*) with slopes of 2.3 $RT/(1-\alpha)nF$ and $-2.3\ RT/\alpha nF$ ($T = 298.15$ K, $R = 8.314$ J mol^{-1} K^{-1}, and $F = 96{,}480$ C mol^{-1}), respectively. Thus, the charge-transfer coefficient (α) was calculated to be 0.47.

$$\log \frac{v_a}{v_c} = \log \frac{\alpha}{1-\alpha} \tag{1}$$

3.5 Electrochemical effective surface area

Figure 7 showed the plots of $Q - t$ and $Q - t^{1/2}$ at bare GCE and $(GQDs/Au)_4$/GCE in 1×10^{-4} mol L^{-1} $K_3[Fe(CN)_6]$ solution containing 1 mol L^{-1} KCl. From the slope of the plot of *Q* versus $t^{1/2}$, the electrochemical effective surface area for bare GCE and $(GQDs/Au)_4$/GCE can be calculated by chronocoulometry using 1×10^{-4} mol L^{-1}

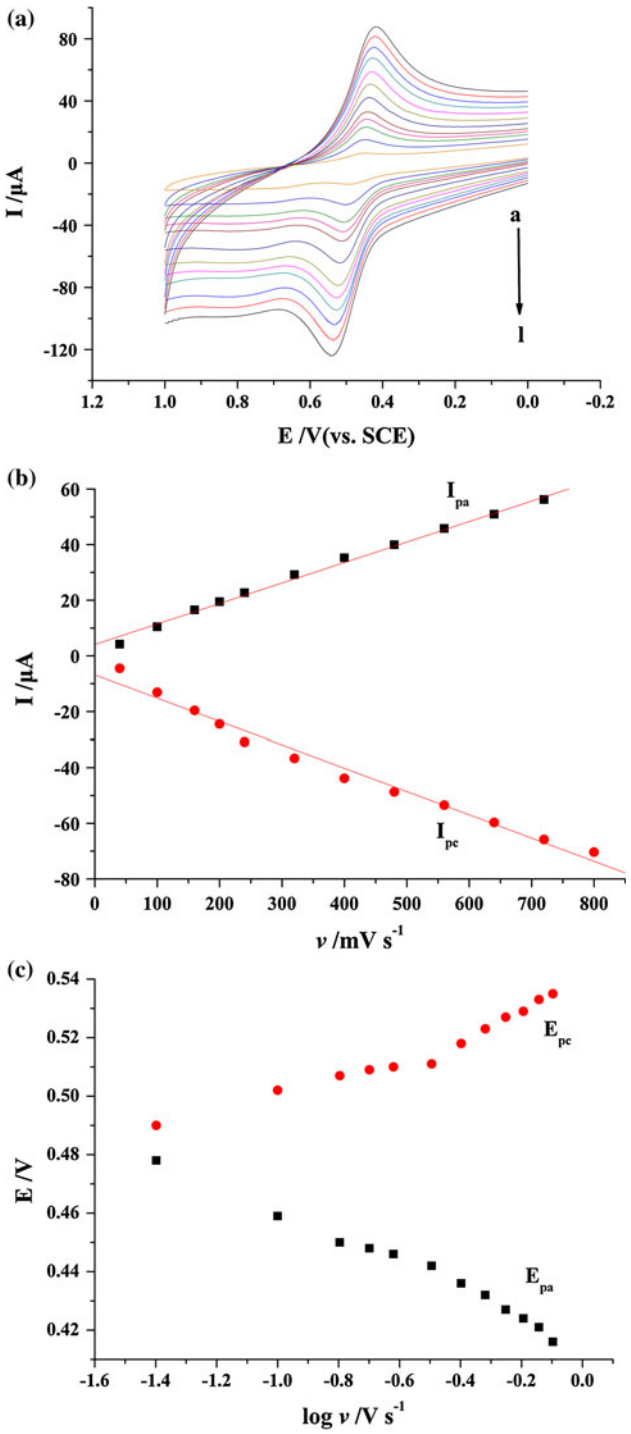

Fig. 6 **a** Cyclic voltammograms of 4.0×10^{-5} mol L^{-1} MG in 0.05 mol L^{-1} H_2SO_4 solution at the $(GQDs/Au)_4$/GCE at different scan rates (from *a* to *l*: 40, 100, 160, 200, 240, 320, 400, 480, 560, 640, 720, and 800 mV s^{-1}). **b** The plot of peak current versus scan rate. **c** The relationship between E_p and the logarithm of scan rate (log *v*)

$K_3[Fe(CN)_6]$ as model complex (the diffusion coefficient D of $K_3[Fe(CN)_6]$ is 7.6×10^{-6} cm^2 s^{-1} [28]) based on Eq. (2) given by Anson [29]:

$$Q(t) = \frac{2nFAcD^{1/2}t^{1/2}}{\pi^{1/2}} + Q_{dl} + Q_{ads} \quad (2)$$

where n is electron transfer number, A is the surface area of the working electrode, c is the concentration of substrate, D is the diffusion coefficient, Q_{dl} is double-layer charge which could be eliminated by background subtraction, and Q_{ads} is adsorption charge. Based on the slope of the linear relationship between Q and $t^{1/2}$, A can be calculated to be 0.093 and 0.460 cm^2 for GCE (Fig. 7 inset a) and $(GQDs/Au)_4$/GCE (Fig. 7 inset b), respectively. The results indicated that the electrode effective surface area was increased after modification of GCE.

3.6 Calibration and limit of detection

Figure 8a showed the DPV curves of MG at various concentrations. The oxidation peak current was proportional to the concentration of MG in the range of 4.0×10^{-7}–1.0×10^{-5} mol L^{-1} with a linear regression equation of $I_{pc} = -2.040 \times 10^6\ c - 5.483$ (μA, mol L^{-1}, $R = 0.992$) (Fig. 8b), and the detection limit was estimated to be 0.1 μmol L^{-1} at a signal-to-noise ratio of 3, indicating an easy method to detect MG was obtained. Hence, it can be concluded that the modified electrode showed excellent sensitivity for MG.

3.7 Determination of MG in real sample

In order to further evaluate the practicality of the proposed method, standard addition method was adopted to estimate the accuracy. The recoveries ranged from 96.25 to 98.00 % as shown in Table 1. Therefore, $(GQDs/Au)_4$/GCE was able to determine the concentration of MG in fish samples.

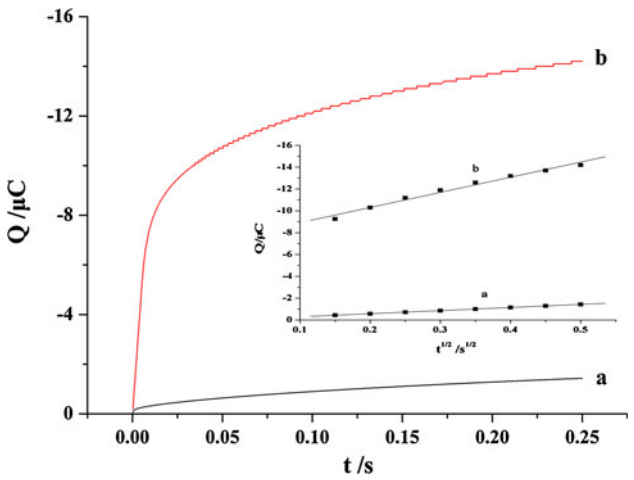

Fig. 7 Plot of Q–t curve of GCE (*a*) and $(GQDs/Au)_4$/GCE (*b*) in 1×10^{-4} mol L^{-1} $K_3[Fe(CN)_6]$ containing 1 mol L^{-1} KCl. *Inset*: plot of $Q - t^{1/2}$ curve at GCE (*a*) and $(GQDs/Au)_4$/GCE (*b*)

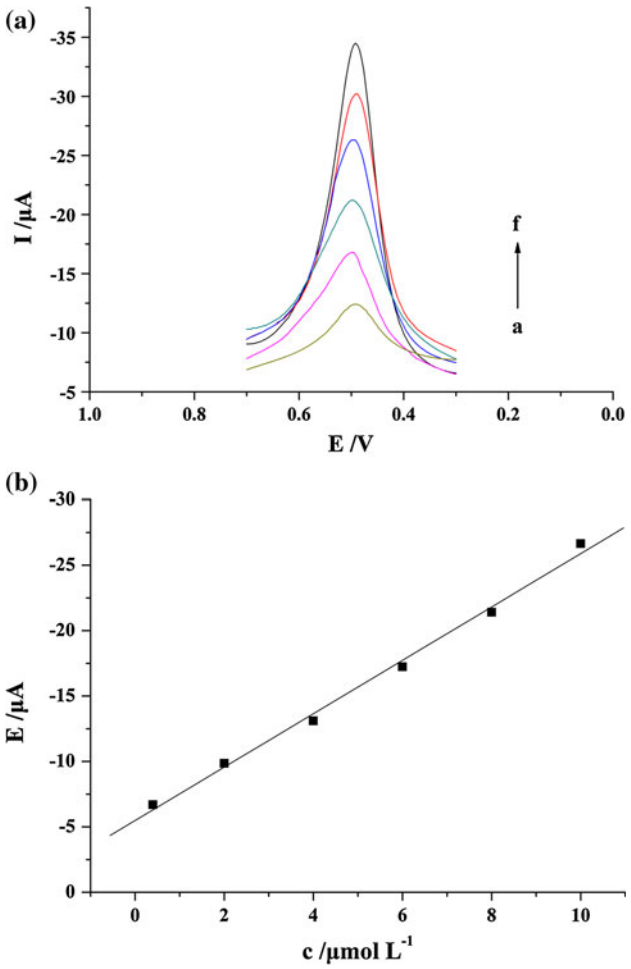

Fig. 8 **a** Differential pulse voltammograms of MG at the $(GQDs/Au)_4$/GCE with various concentrations (from *a* to *f*: 4.0×10^{-7}, 2.0×10^{-6}, 4.0×10^{-6}, 6.0×10^{-6}, 8.0×10^{-6}, and 1.0×10^{-5} mol L^{-1}). **b** Calibration curve for MG at $(GQDs/Au)_4$/GCE

3.8 Stability, reproducibility, and selectivity of the modified electrodes

The stability and reproducibility were evaluated by measuring the electrochemical response of 4.0×10^{-6} mol L^{-1}

Table 1 Recovery values of MG obtained for three salmon samples ($n = 3$)

Samples	Added (μmol L^{-1})	Found (μmol L^{-1})	Recovery (%)	RSD (%)
1	4.0	3.85	96.25	4.2
2	4.0	3.92	98.00	3.2
3	4.0	3.90	97.50	5.4

MG at the $(GQDs/Au)_4$/GCE. The modified electrode retained 92 % of its initial response after it was kept in refrigerator at 4 °C for 10 days, which indicated that the modified electrode had good stability. The reproducibility was investigated by five parallel modified electrodes. The relative standard deviation was 6.90 %, which suggested that the $(GQDs/Au)_4$/GCE displayed good reproducibility.

To evaluate the selectivity of the fabricated electrode, the influence of some complexes and inorganic ions was examined in 0.05 mol L^{-1} H_2SO_4 solution containing 4.0×10^{-6} mol L^{-1} MG. The results suggested that 200-fold concentration of ascorbic acid, uric acid, dopamine, caffeine, vitamin E, xanthine, hypoxanthine, and leukomalachite green had no influence on the signals of MG with deviations below 10 %. Additionally, some inorganic ions such as 400-fold concentration of Na^+, Ca^{2+}, Mg^{2+}, Fe^{3+}, Al^{3+}, Zn^{2+}, Cu^{2+}, Cl^-, SO_4^{2-}, PO_4^{3-}, and NO_3^- had no influence on MG determination.

4 Conclusions

In this paper, a new graphene quantum dots–gold nanoparticles multilayers–modified electrode was successfully fabricated to detect MG. The electrode effective surface area was increased four times after modification. Owing to the synergistic effects of GQDs and Au nanoparticles, the oxidation peak potential of MG was decreased, and the oxidation peak current was increased. Furthermore, by layer-by-layer methods, the oxidation peak current at the $(GQDs/Au)_n$/GCE was increased by 132 % in 1.0×10^{-5} mol L^{-1} MG. The application of this modified electrode in analysis of real samples was also evaluated with good performance. This proposed method was a promising electrochemical approach for tracing MG.

Acknowledgments This work was supported by the National Natural Science Foundation of China (No. 21075078, 21105056) and the Natural Science Foundation of Shandong province, China (ZR2010BM005, ZR2011BQ001).

References

1. Fernandes C, Lalitha VS, Rao KV (1991) Enhancing effect of malachite green on the development of hepatic pre-neoplastic lesions induced by N-nitrosodiethylamine in rats. Carcinogenesis 12(5):839–845
2. Rao K (1995) Inhibition of DNA synthesis in primary rat hepatocyte cultures by malachite green: a new liver tumor promoter. Toxicol Lett 81(2):107–113
3. Gouranchat C (2000) Malachite green in fish culture (state of the art and perspectives). Bibliographic study. Ecole natl Veterinaire ENVT, Nantes (France) 142:2000
4. Andersen WC, Turnipseed SB, Roybal JE (2006) Quantitative and confirmatory analyses of malachite green and leucomalachite green residues in fish and shrimp. J Agric Food Chem 54(13):4517–4523
5. Rushing LG, Thompson HC Jr (1997) Simultaneous determination of malachite green, gentian violet and their leuco metabolites in catfish or trout tissue by high-performance liquid chromatography with visible detection. J Chromatogr B Biomed Sci Appl 688(2):325–330
6. Mitrowska K, Posyniak A, Zmudzki J (1089) Determination of malachite green and leucomalachite green in carp muscle by liquid chromatography with visible and fluorescence detection. J Chromatogr A 1089(1):187–192
7. Xing W, He L, Yang H, Sun C, Li D, Yang X, Li Y, Deng A (2009) Development of a sensitive and group-specific polyclonal antibody-based enzyme-linked immunosorbent assay (ELISA) for detection of malachite green and leucomalachite green in water and fish samples. J Sci Food Agric 89(13):2165–2173
8. Yang MC, Fang JM, Kuo TF, Wang DM, Huang YL, Liu LY, Chen PH, Chang TH (2007) Production of antibodies for selective detection of malachite green and the related triphenylmethane dyes in fish and fishpond water. J Agric Food Chem 55(22):8851–8856
9. Bilandžić N, Varenina I, Kolanović BS, Oraić D, Zrnčić S (2012) Malachite green residues in farmed fish in Croatia. Food Control 26(2):393–396
10. Yi H, Qu W, Huang W (2008) Electrochemical determination of malachite green using a multi-wall carbon nanotube modified glassy carbon electrode. Microchim Acta 160(1):291–296
11. Novoselov K, Geim A, Morozov S, Jiang D, Zhang Y, Dubonos S, Grigorieva I, Firsov A (2004) Electric field effect in atomically thin carbon films. Science 306(5696):666–669
12. Chen D, Tang L, Li J (2010) Graphene-based materials in electrochemistry. Chem Soc Rev 39(8):3157–3180
13. Moradi-Monfared S, Krishnamurthy V, Cornell B (2012) A molecular machine biosensor: construction, predictive models and experimental studies. Biosens Bioelectron 34(1):261–266
14. Zhao J, Chen G, Zhu L, Li G (2011) Graphene quantum dots-based platform for the fabrication of electrochemical biosensors. Electrochem Commun 13(1):31–33
15. Razmi H, Mohammad-Rezaei R (2012) Graphene quantum dots as a new substrate for immobilization and direct electrochemistry of glucose oxidase: application to sensitive glucose determination. Biosens Bioelectron 41(1):498–504
16. Zhou K, Zhu Y, Yang X, Luo J, Li C, Luan S (2010) A novel hydrogen peroxide biosensor based on Au–graphene–HRP–chitosan biocomposites. Electrochim Acta 55(9):3055–3060
17. Chang H, Shiu KK, Jiang H, Zhu Y, Wang J, Li Q, Chen B, Wang X (2013) Layer-by-layer assembly of graphene, Au and poly (toluidine blue O) films sensor for evaluation of oxidative stress of tumor cells elicited by hydrogen peroxide. Biosens Bioelectron 41(15):789–794
18. Li LL, Ji J, Fei R, Wang CZ, Lu Q, Zhang JR, Jiang LP, Zhu JJ (2012) A facile microwave avenue to electrochemiluminescent two-color graphene quantum dots. Adv Funct Mater 22(14):2971–2979
19. Xu Y, Bai H, Lu G, Li C, Shi G (2008) Flexible graphene films via the filtration of water-soluble noncovalent functionalized graphene sheets. J Am Chem Soc 130(18):5856–5857
20. Arcos D, Lopez-Noriega A, Ruiz-Hernandez E, Terasaki O, Vallet-Regi M (2009) Ordered mesoporous microspheres for bone grafting and drug delivery. Chem Mater 21(6):1000–1009
21. Wan Q, Wang X, Yang N (2006) Poly (malachite green) film: electrosynthesis, characterization, and sensor application. Polymer 47(22):7684–7692
22. Wang X, Yang N, Wan Q (2007) Catalytic capability of poly (malachite green) films based electrochemical sensor for oxidation of dopamine. Sens Actuators B Chem 128(1):83–90

23. Umasankar Y, Periasamy AP, Chen SM (2010) Poly (malachite green) at nafion doped multi-walled carbon nanotube composite film for simple aliphatic alcohols sensor. Talanta 80(3):1094–1101
24. Chen SM, Chen JY, Thangamuthu R (2007) Electrochemical preparation of poly(malachite green) film modified Nafion-coated glassy carbon electrode and its electrocatalytic behavior towards NADH, dopamine and ascorbic acid. Electroanalysis 19(14): 1531–1538
25. Umasankar Y, Periasamy AP, Chen SM (2011) Electrocatalysis and simultaneous determination of catechol and quinol by poly(malachite green) coated multiwalled carbon nanotube film. Anal Biochem 411(1):71–79
26. Fang C, Tang XR, Zhou XY (1999) Preparation of poly(malachite green) modified electrode and the determination of dopamine and ascorbic acid. Anal Sci 15(1):41–46
27. Laviron E (1979) General expression of the linear potential sweep voltammogram in the case of diffusionless electrochemical systems. J Electroanal Chem Interfacial Electrochem 101(1):19–28
28. Adams R (1969) Electrochemistry at solid electrodes. M. Dekker, New York, pp 115–139
29. Anson F (1964) Application of potentiostatic current integration to the study of the adsorption of cobalt (III)-(ethylenedinitrilo (tetraacetate) on mercury electrodes. Anal Chem 36(4):932–934